Liquid−Liquid Equilibrium for Ternary Systems Containing Ethyl Esters, Anhydrous Ethanol and Water at 298.15, 313.15, and 333.15 K

Luis A. Follegatti-Romero,[†] Marcelo Lanza,[†] Fabio R. M. Batista,[†] Eduardo A. C. Batista,[†] Mariana B. Oliveira,[‡] João A. P. Coutinho,[‡] and Antonio J. A. Meirelles*,[†]

ExTrAE, Laboratory of Extraction, Applied Thermodynamics and Equilibrium, Department of Food Engineering, Faculty of Food Engineering, University of Campinas—UNICAMP, 13083-862, Campinas, SP, Brazil, and CICECO, Chemistry Department, University of Aveiro, 3810-193, Aveiro, Portugal

The most common method used for purifying biodiesel is washing with water. During the biodiesel washing process, two phases are formed, a water-rich phase and an ester-rich one. For this reason, knowledge of the corresponding phase equilibrium is an important step in optimizing the final purification of biodiesel. The objective of this work was to investigate the liquid−liquid equilibrium related to some esters of interest in the production of ethylic biodiesel, in particular the equilibrium data for systems containing ethyl laurate/ethyl myristate + ethanol + water at 298.15, 313.15, and 333.15 K. The data obtained were correlated with the cubic-plus-association equation of state (CPA EoS). It was shown that this model was able to provide a very good description of the phase diagrams of the systems studied.

Introduction

Ethylic biodiesel, composed of fatty acid ethyl esters (FAEE) and produced by transesterification of vegetable oils with bioethanol, is a biofuel entirely based on renewable agricultural sources. In contrast to methylic biodiesel, produced using methanol typically obtained from natural gas or coal, ethylic biodiesel tends to be carbon neutral with respect to the environmental issue.[1] Ethylic biodiesel also shows the following advantages in comparison to its methylic counterpart: it exhibits lower pour and cloud points and better storage properties.[2] On the other hand, the production of biodiesel by ethanolysis appears to consume more energy, and recovery of the ethyl esters from the reaction product is more difficult.[2] Several vegetable oils have been successfully used as renewable sources for biodiesel production, including those rich in lauric and myristic acids, such as palm kernel (South-East Asia, Nigeria, Colombia, and Ecuador) and babassu oils (Brazil).[3−5]

Three main steps are usually necessary to convert vegetable oils into FAEE. The first step is a pretreatment of the vegetable oil, carried out with the main purpose of removing free fatty acids that could interfere with the appropriate reaction path. The second is the reactive step, also denominated the transesterification reaction, and the third is a sequence of purification procedures aimed at obtaining a final product that conforms to the legislation standards. During the transesterification step palm kernel and babassu oils are mainly transformed into ethyl laurate and ethyl myristate, since lauric and myristic acids represent more than 60% of the total amount of fatty acids.[6]

The transesterification reaction can generate very pure ethylic esters, but a purification step is usually required in order to separate the esters obtained from the glycerol, the excess of alcoholic reagent, the residual acylglycerols that did not react, and any contaminants introduced into the process together with the reagents, such as other minor fatty compounds. The purity grade of biodiesel has an important influence on its fuel properties, so it must be almost free of water, alcohol, glycerol, catalyst, and acylglycerols. The washing of biodiesel is used to remove the residues of ethanol, glycerol, catalyst, and soaps.[7,8] Karaosmanoğlu et al.[9] tested different alternatives for purifying biodiesel and selected washing with hot distilled water at 323.15 K as the best refining option, capable of producing a biofuel with purity of around 99%.

Despite the importance of this purification step, experimental equilibrium data on the two phases formed during biodiesel washing are scarce, especially in the case of ethylic biodiesel. Some research groups have recently published experimental results on the phase behavior of the reactants and products present in the biodiesel reaction.[10−13]

In this work, liquid−liquid equilibrium data for the following ternary systems of interest in the production of ethylic biodiesel were investigated: ethyl laurate + ethanol + water and ethyl myristate +ethanol + water at 298.15 ± 0.1, 313.15 ± 0.1, and 333.15 ± 0.1 K. The CPA EoS was used to correlate the measured phase diagrams. This model has already been successfully applied to mixtures similar to those investigated in the present work, such as water−alcohol[14] and methyl oleate−glycerol−methanol[15] mixtures.

Experimental Section

Materials. The ethyl laurate and ethyl myristate used in this work were purchased from Tecnosyn (Cajamar/SP, Brazil), and their mass purities were 99.3 and 99.5%, respectively. The solvents used were anhydrous ethanol from Merck, with a mass purity of 99.9%, and acetonitrile from Vetec, with a mass purity of 99.8%.

Quantification of the ethyl esters and ethanol was carried out in a Shimadzu (GC-17A) capillary gas chromatograph system with programmable pneumatics and a flame ionization detector (FID). A DB-WAX capillary column (0.25 μm, 30 m × 0.25 mm i.d) from J&W Scientific (Rancho Cordoba, CA, USA) was used, and the carrier gas was helium from White Martins, with a mass purity of 99.9%. The water content of both phases was determined by Karl Fischer titration using a model 701 Metrohm apparatus equipped with a 5 mL buret. The Karl Fischer reagent used in the titration was from Merck.

Apparatus and Procedures. The liquid−liquid equilibrium data for the systems containing laurate/ethyl myristate + ethanol

* To whom correspondence should be addressed. Tel.: +55 19 3521 4037. Fax: +55 19 3521 4027. E–mail: tomze@fea.unicamp.br.
[†] University of Campinas—UNICAMP.
[‡] University of Aveiro.

10.1021/ie101611j

+ water were determined at 298.15 ± 0.1, 313.15 ± 0.1, and 333.15 ± 0.1 K. The binodal curves for both ternary systems at each temperature were determined by the cloud−point method following the same procedures described by Lanza et al.[16] The tie lines were determined using glass test tubes with screw caps (32 mL). Known quantities of each component were weighed on an analytical balance with a precision of 0.0001 g (Precisa, model XT220A) and added directly to the glass test tubes. The mixture of ethyl ester, ethanol, and water was maintained under intensive agitation for 10 min at constant temperature and pressure using a test tube shaker (Phoenix, model AP 56). The ternary mixture was then left at rest for 24 h in a thermostatic water bath at the desired temperature, until two separate, transparent liquid phases were clearly observed. At the end of the experiment, samples were taken separately from the upper and bottom phases using syringes containing previously weighed masses of acetonitrile, so as to guarantee an immediate dilution of the samples and avoid further separation into two liquid phases at ambient temperature.

The samples from the two phases were analyzed by gas chromatography (GC). The detector and injector temperatures were 553 and 523 K, respectively. The column oven was maintained at 313.15 K for 8 min and subsequently submitted to the following heating program: from 313.15 to 473.15 K at a rate of 20 K·min^{-1}, maintained at 473.15 K for 8 min; from 473.15 to 483.15 K at a rate of 10 K·min^{-1}; and finally maintained at 483.15 K for 2 min. The absolute pressure of the column was approximately 114 kPa, the carrier gas flowed at a rate of 1.6 mL·min^{-1}, the linear velocity was 34 cm·s^{-1}, and the sample injection volume was 1.0 μL.

The quantitative determination was carried out using calibration curves (external calibration) obtained using standard solutions for each system component: ethyl laurate, ethyl myristate, and ethanol. These compounds were diluted with acetonitrile in the concentration range from 0.5 to 100 mg/mL. The experimental data for each tie line were replicated at least three times, and the values reported in the present work are the average ones. The mass fractions of ethyl esters and ethanol were determined from the areas of the corresponding GC chromatographic peaks, adjusted by the response factors obtained by previous calibration. The water mass fractions were also determined at least three times using the Karl Fisher titration, and the values reported are the average ones.

The distribution coefficients and the solvent selectivity were calculated according to eqs 1 and 2, respectively, using the experimental compositions of both phases.

$$K_{d3} = \frac{w_3^{WP}}{w_3^{EP}} \tag{1}$$

$$S_{3/i} = \frac{K_{d3}}{K_{di}} \tag{2}$$

where k_{d3} is the distribution coefficient for ethanol, w_3 is its mass fraction in the water (WP) or ester (EP) phases, respectively, and $S_{3/i}$ stands for the solvent selectivity. The solvent selectivity reflects its effectiveness in separating ethanol from the ester phase ($i = 1$ for ethyl laurate or $i = 2$ for ethyl myristate).

Thermodynamic Modeling. The modeling of polar and highly nonideal systems in wide ranges of temperature and pressure requires the use of association equations of state that explicitly take into account specific interactions between like (self-association) and unlike (cross-association) molecules. One of these equations is the cubic-plus-association (CPA) equation of state, proposed by Kontogeorgis and co-workers,[17−19] that combines a physical contribution from a cubic equation of state, in this work the Soave−Redlich−Kwong (SRK) one, with an association term accounting for intermolecular hydrogen bonding and solvation effects,[20−22] originally proposed by Wertheim and used in other association equations of state such as SAFT.[23]

It can be expressed in terms of the compressibility factor as

$$Z = Z^{phys.} + Z^{assoc} = \frac{1}{1 - b\rho} - \frac{a\rho}{RT(1 + b\rho)} - \frac{1}{2}\left(1 + \rho\frac{\partial \ln g}{\partial \rho}\right)\sum_i x_i \sum_{A_i}(1 - X_{A_i}) \tag{3}$$

where a is the energy parameter, b the covolume parameter, ρ the molar density, g a simplified hard-sphere radial distribution function, X_{A_i} the mole fraction of pure component i not bonded at site A, and x_i the mole fraction of component i.

The pure component energy parameter, a, is obtained from a Soave-type temperature dependency:

$$a(T) = a_0[1 + c_1(1 - \sqrt{T_r})]^2 \tag{4}$$

where a_0 and c_1 are regressed (simultaneously with b) from pure component vapor pressure and liquid density data.

When CPA is extended to mixtures, the energy and covolume parameters of the physical term are calculated by employing the conventional van der Waals one-fluid mixing rules:

$$a = \sum_i \sum_j x_i x_j \quad a_{ij}a_{ij} = \sqrt{a_i a_j}(1 - k_{ij}) \tag{5}$$

$$b = \sum_i x_i b_i \tag{6}$$

X_{A_i} is related to the association strength $\Delta^{A_iB_j}$ between sites belonging to two different molecules and is calculated by solving the following set of equations:

$$X_{A_i} = \frac{1}{1 + \rho\sum_j x_j \sum_{B_j} X_{B_j}\Delta^{A_iB_j}} \tag{7}$$

where

$$\Delta^{A_iB_j} = g(\rho)\left[\exp\left(\frac{\varepsilon^{A_iB_j}}{RT}\right) - 1\right]b_{ij}\beta^{A_iB_j} \tag{8}$$

where $\varepsilon^{A_iB_j}$ and $\beta^{A_iB_j}$ are the association energy and the association volume, respectively.

The simplified radial distribution function, $g(\rho)$, is given by[24]

$$g(\rho) = \frac{1}{1 - 1.9\eta} \quad \text{where } \eta = \frac{1}{4}b\rho \tag{9}$$

For nonassociating components, such as esters, CPA has three pure component parameters in the cubic term (a_0, c_1, and b), while for associating components, such as water and alcohols, it has two additional parameters in the association term (ε and β). In both cases, the parameters are regressed simultaneously from the vapor pressure and liquid density data. The objective function to be minimized is the following:

$$OF = \sum_i^{NP}\left(\frac{P_i^{exptl} - P_i^{calcd}}{P_i^{exptl}}\right)^2 + \sum_i^{NP}\left(\frac{\rho_i^{exptl} - \rho_i^{calcd}}{\rho_i^{exptl}}\right)^2 \tag{10}$$

For a binary mixture composed solely of nonassociating compounds, the binary interaction parameter, k_{ij} (eq 5), is the only adjustable parameter.

When CPA is used for mixtures containing two self-associating compounds, combining rules for the association term are required,[24,25] and in this work, the Elliott combining rule (ECR)[25] was used:

$$\Delta^{A_iB_j} = \sqrt{\Delta^{A_iB_i}\Delta^{A_jB_j}} \tag{11}$$

The Elliot combining rule provided very good results in modeling the phase equilibrium of several systems of interest for the production of biodiesel, such as, for example, the liquid−liquid equilibrium (LLE) of water + fatty acid systems[26] and the vapor−liquid equilibrium (VLE) of glycerol + alcohol systems.[27]

Solvation can occur in some systems containing self-associating and non-self-associating compounds, as in the case of the ester + water or ethanol mixtures investigated in this work. For this type of system, the solvation phenomena are considered as a cross-association by the CPA EoS, where the cross-association energy ($\varepsilon^{A_iB_j}$) is considered to be half the value of the association energy for the self-associating component and the cross-association volume ($\beta^{A_iB_j}$) is left as an adjustable parameter, fitted to the equilibrium data. This approach, proposed by Folas et al.,[28] was successfully applied to model the phase equilibrium of several water + aromatic[29] and water + fatty acid ester[30] systems and to correlate the water solubility in biodiesels.[30] In these cases, the following objective function was minimized to estimate the parameters k_{ij} and $\beta^{A_iB_j}$:

$$\mathrm{OF} = \sum_{i}^{\mathrm{NP}} \left(\frac{x_i^{\mathrm{calcd}} - x_i^{\mathrm{exptl}}}{x_i^{\mathrm{exptl}}} \right)^2 \tag{12}$$

where single-phase or all-phase data can be selected during optimization of the parameter. The association term depends on the number and type of association sites. According to the nomenclature of Huang and Radosz,[31] for alcohols, the two-site (2B) association scheme is applied, which proposes that hydrogen bonding occurs between the hydroxyl hydrogen and one of the lone pairs of electrons from the oxygen atom of another alcohol molecule. For the ester family, a single association site is considered that can cross-associate with self-associating molecules. For water, a four-site (4C) association scheme is adopted, considering that hydrogen bonding occurs between the two hydrogen atoms and the two lone pairs of electrons of the oxygen of the water molecule.

The average deviations (AD) between the experimental compositions and those estimated by the CPA EoS were calculated according to

$$\mathrm{AD} = \sqrt{\frac{\sum_{n}^{N}\sum_{i}^{R}[(w_{i,n}^{\mathrm{WP,exptl}} - w_{i,n}^{\mathrm{WP,calcd}})^2 + (w_{i,n}^{\mathrm{EP,exptl}} - w_{i,n}^{\mathrm{EP,calcd}})^2]}{2NR}} \tag{13}$$

where AD is the average deviation for each system, N is the total number of tie lines of the corresponding system, R is the

Table 1. Experimental Liquid−Liquid Equilibrium Data for the Ternary Systems Containing Ethyl Ester (*i*) + Anhydrous Ethanol (3) + Water (4) at 298.15 ± 0.1, 313.15 ± 0.1, and 333.15 ± 0.1 K

		overall composition			water-rich phase			ester-rich phase				
ethyl ester (*i*)	T (K)	100 w_i	100 w_3	100 w_4	100 w_i	100 w_3	100 w_4	100 w_i	100 w_3	100 w_4	K_{d3}[a]	$S_{3/1}$[b]
laurate (1)	298.15	19.981	59.919	20.100	12.950	64.407	22.643	71.266	24.313	4.421	2.649	14.5
		24.695	50.560	24.745	3.411	63.025	33.564	82.086	15.829	2.085	3.982	95.8
		31.364	37.269	31.367	0.497	51.614	47.889	90.119	8.765	1.116	5.889	1067.7
		37.794	25.661	36.546	0.059	39.817	60.124	93.233	5.955	0.812	6.686	10565.8
		39.141	21.817	39.043	0.032	34.090	65.878	95.323	4.137	0.540	8.240	24546.4
		44.751	11.441	43.808	0.004	17.496	82.500	97.159	2.499	0.342	7.001	170057.4
		51.216	0.000	48.784	0.003	0.000	99.997	99.790	0.000	0.210		
	313.15	24.705	50.55	24.743	5.468	61.753	32.780	77.534	19.107	3.359	3.232	45.8
		31.358	37.29	31.355	0.825	52.240	46.935	87.564	10.492	1.945	4.979	528.4
		37.784	25.68	36.535	0.219	41.658	58.123	92.344	6.106	1.550	6.822	2876.7
		39.138	21.82	39.044	0.183	34.424	65.393	94.354	4.453	1.193	7.731	3985.8
		44.758	11.43	43.817	0.079	18.246	81.676	96.050	2.919	1.031	6.251	7599.8
		52.133	0.00	47.867	0.043	0.000	99.957	99.161	0.000	0.839		
	333.15	24.720	50.543	24.737	6.500	63.116	30.384	71.599	22.671	5.730	2.784	30.6
		31.346	37.307	31.347	0.985	52.541	46.474	85.282	12.201	2.517	4.306	372.8
		35.889	28.348	35.763	0.496	42.304	57.200	88.990	9.000	2.010	4.700	843.3
		39.110	21.869	39.021	0.205	35.236	64.559	91.867	6.449	1.683	5.464	2448.5
		44.748	11.434	43.819	0.090	20.011	79.899	94.647	3.765	1.588	5.315	5589.4
		49.022	0.000	50.978	0.050	0.000	99.950	98.980	0.000	1.020		
myristate (2)	298.15	18.798	62.257	18.945	6.010	72.466	21.524	73.536	23.343	3.121	3.104	37.9
		23.183	53.477	23.340	2.431	65.162	32.407	83.759	14.392	1.849	4.528	156.0
		30.112	39.431	30.457	0.370	54.139	45.491	90.462	8.616	0.922	6.284	1536.2
		35.077	29.810	35.113	0.129	42.971	56.900	92.960	6.279	0.761	6.844	4931.6
		39.229	21.532	39.239	0.103	33.467	66.430	94.499	4.934	0.567	6.783	6223.1
		44.564	10.341	45.095	0.092	17.008	82.900	98.520	1.020	0.460	16.675	17856.2
		48.741	0.000	51.259	0.070	0.000	99.930	99.740	0.000	0.260		
	313.15	23.155	53.492	23.353	2.945	66.051	31.004	80.607	16.365	3.027	4.036	110.4
		31.319	38.748	29.933	0.829	54.352	44.819	88.819	9.265	1.917	5.866	628.5
		35.081	29.808	35.111	0.200	43.554	56.246	91.986	6.994	1.020	6.227	2864.1
		39.116	21.665	39.219	0.115	33.643	66.242	94.024	5.210	0.766	6.457	5279.5
		55.341	8.337	36.322	0.100	17.489	82.411	98.390	1.110	0.500	15.756	15502.1
		48.718	0.000	51.282	0.075	0.000	99.925	99.720	0.000	0.280		
	333.15	23.192	53.483	23.325	7.258	62.135	30.607	58.636	34.468	6.895	1.803	14.5
		30.109	39.435	30.456	1.299	54.447	44.253	73.114	21.500	5.386	2.532	142.5
		35.114	29.862	35.024	0.242	43.767	55.991	84.579	12.480	2.941	3.507	1225.6
		39.491	21.014	39.495	0.128	33.666	66.206	92.140	5.810	2.050	5.794	4171.1
		44.559	10.353	45.088	0.012	17.706	82.282	95.129	2.890	1.981	6.127	48568.4
		48.741	0.000	51.259	0.080	0.000	99.920	99.110	0.000	0.890		

[a] K_{d3} is the ethanol distribution coefficient according to eq 1. [b] $S_{3/1}$ is the solvent selectivity according to eq 2.

Table 2. Deviations for the Global Mass Balance of the Phase Compositions

system	$100\delta^a$	system	$100\delta^a$
ethyl laurate + ethanol + water at 298.15 K	0.20	ethyl myristate + ethanol + water at 298.15 K	0.35
ethyl laurate + ethanol + water at 313.15 K	0.16	ethyl myristate + ethanol + water at 313.15 K	0.11
ethyl laurate + ethanol + water at 333.15 K	0.43	ethyl myristate + ethanol + water at 333.15 K	0.27

[a] Relative deviation of the overall mass balance, calculated by $\delta = (1/N)\sum_n^N |(m^{EP} + m^{WP} - m^{OS})/m^{OS}|$, where m^{EP} is the calculated mass of the ester-rich phase, m^{WP} is the corresponding value of the water-rich phase, m^{OS} is the total mass of the system, and n is the tie line number.

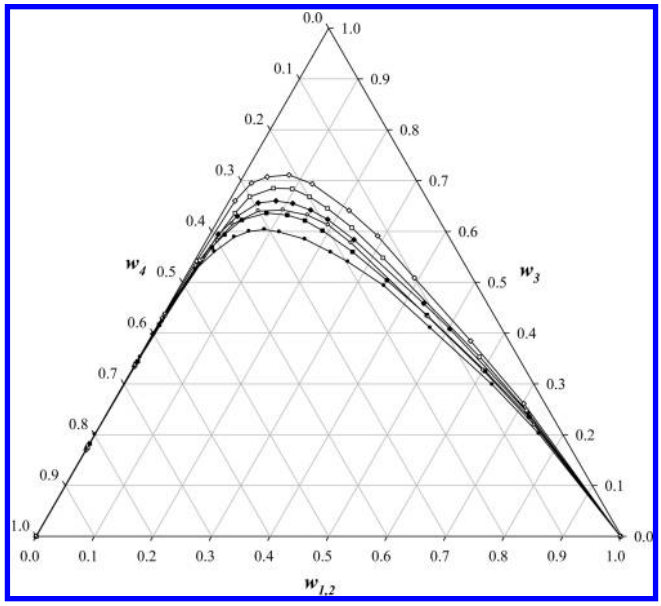

Figure 1. Binodal curves of ethyl laurate (1) + ethanol (3) + water (4) [(♦) 298.15, (■) 313.15, and (●), 333.15 K] and ethyl myristate (2) + ethanol (3) + water (4) [(◇) 298.15, (□) 313.15, and (○) 333.15 K].

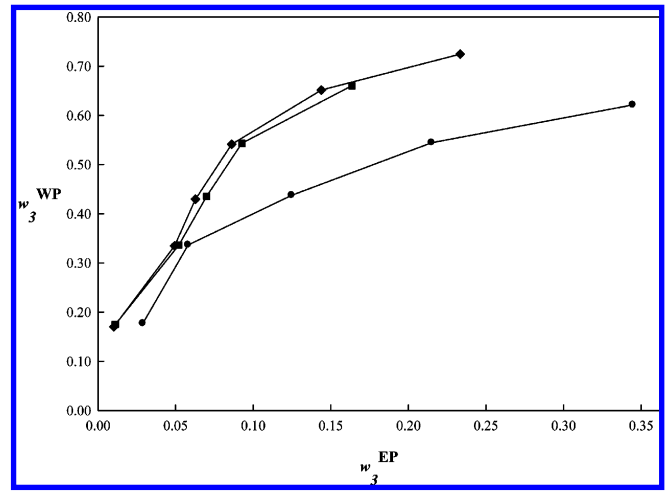

Figure 2. Distribution diagram for ethyl myristate (2) + ethanol (3) + water (4): (♦) 298.15, (■) 313.15, and (●) 333.15 K.

total number of components ($R = 3$), w is the mass fraction, i is the component, the subscript n stands for the tie line number, and the superscripts exptl and calcd refer to the experimental and calculated compositions.

Results and Discussion

Table 1 shows the experimental equilibrium data given in percentage by mass. The type A standard uncertainties[32] of the equilibrium compositions ranged from 0.0005 to 0.0882% by mass for ethyl esters, from 0.0029 to 0.8378% for ethanol, and from 0.0888 to 0.8343% for water, with the lowest figures associated with the lowest mass fractions within the composition range investigated.

On the basis of the total system mass and of the phase and overall compositions, the mass balances were checked according to the procedure suggested by Marcilla et al.[33] and recently applied to fatty systems by da Silva et al.[34] According to this procedure, the masses of both liquid phases were calculated and checked against the total initial mass used in the experimental runs. The average results obtained for the mass balance deviations of each set of experimental data are shown in Table 2. In all cases, the values were lower than 0.50%, which indicates the good quality of the experimental data.

Figure 1 shows the binodal curves for the ethyl laurate and ethyl myristate systems. (The experimental data used are presented in the Supporting Information, Table S1.) The size of the phase splitting region only decreased slightly with the increase in temperature. The same behavior was observed for both systems, but in the case of ethyl myristate the size of the phase splitting region was larger. The distribution diagram for ethanol in the ethyl myristate system is shown in Figure 2. The ethanol mass fraction in the aqueous phase was much larger than in the ester phase so that its distribution coefficient was, in most cases, above 1.8 for both systems (see Table 1). Considering that the ester mass fraction in the aqueous phase was usually low, the solvent selectivity was very high, in most cases above 100 (see Table 1). These results indicate that washing with water is a very effective way of extracting ethanol from the ester phase generated at the end of the ethanolysis reaction, without losing any significant amount of biodiesel to the extract phase.

The CPA EoS was previously used with success for the description of LLE in systems such as methyl oleate + methanol + glycerol, fatty acid ester + ethanol + glycerol,and methyl ricinoleate + methanol + glycerol, using the same temperature-independent binary interaction and cross-association parameters.[35] Given the accuracy, predictivity, and simplicity provided by the CPA EoS in modeling complex multicomponent associating systems, this equation was selected to describe the LLE of the ternary mixtures studied here.

To apply the CPA EoS to model the phase equilibrium of multicomponent systems, the CPA pure compound parameters must be estimated using a simultaneous regression of the vapor pressure and liquid density data. Nonassociating compounds such as fatty acid esters and self-associating compounds such as ethanol and water are present in these systems. The five CPA pure compound parameters for water were previously established,[36] considering the 4C scheme for water, and were used in modeling the phase equilibrium of several water-containing systems.[26,27,29,30] The three CPA parameters for esters were proposed in a previous work,[30] and it was shown that the a_0, c_1, and b CPA parameters followed the same trend with the ester carbon number. Correlations for the estimation of these parameters with new compounds were proposed, enabling the estimation of the CPA pure compound parameters in the absence of liquid density and vapor pressure data. In a previous work,[37] the CPA parameters for ethyl laurate and ethyl myristate were estimated from these correlations and applied for the prediction

Table 3. CPA Pure Compound Parameters and Critical Temperatures

compound	T_c (K)	a_0 (J·m³·mol⁻²)	c_1	$b \times 10^5$ (m³·mol⁻¹)	ε (J·mol⁻¹)	β	100AAD[a] P	100AAD[a] ρ
ethyl laurate[37,38]	719.1	8.23	1.44	30.18				4.29
ethyl myristate[37,38]	744.3	9.52	1.54	34.54				6.99
ethanol[39]	514.7	0.68	0.94	4.75	21336	0.0190	0.35	0.51
water[36]	647.3	0.12	0.67	1.45	16655	0.0692	1.72	0.82

[a] AAD is the average absolute deviation calculated by $\mathbf{AAD} = (1/N)\sum_{i=1}^{NP} |(\text{exptl}_i - \text{calcd}_i)/\text{exptl}_i|$.

Table 4. Binary Interaction and Cross-Association Parameters Used To Model Ternary Systems LLE

k_{ij}(ethyl laurate+ethanol)	−0.083	β_{ij}(ethyl laurate/ethyl myristate+ethanol)[40]	0.100
k_{ij}(ethyl laurate+water)	−0.172	β_{ij}(ethyl laurate/ethyl myristate+water)[30]	0.201
k_{ij}(ethyl myristate+ethanol)	−0.094	k_{ij}(ethanol+water)	−0.100
k_{ij}(ethyl myristate+water)	−0.155		

of the VLE of the ethyl laurate/ethyl myristate + alcohol systems at near or supercritical conditions.

Recently, new density data appeared for these ethyl esters,[38] and it is now possible to evaluate the predictive capability of the estimated CPA pure compound parameters. As seen in Table 3, where average absolute deviations are presented for the ethyl esters densities, the CPA EoS is able to correctly predict that property.

The five CPA parameters for ethanol were established previously, while performing a systematic study on the pure compound parameters for the *n*-alcohol family from methanol to *n*-eicosanol, using the 2B association scheme.[39] These parameters were used for the description of the LLE of ternary systems constituted of fatty esters, ethanol, and glycerol,[35] of the VLE of the glycerol + ethanol system[27] and of the VLE of fatty acid ester + ethanol systems at atmospheric pressure[40] and at near or supercritical conditions.[37] The pure compound CPA parameters used in this work can be seen in Table 3 along with the deviations obtained for liquid densities and vapor pressures.

The description of multicomponent systems requires the estimation of binary parameters from experimental data. Cross-association parameters, β_{ij}'s, between ethyl laurate/ethyl myristate and water, and between ethyl laurate/ethyl myristate and ethanol, were previously established by Oliveira et al.[30,40] while modeling the LLE of water + fatty acid ester systems and the VLE of ethanol + fatty acid ester systems. Taking advantage of the transferability of the CPA parameters, these β_{ij}'s were applied to the description of the phase diagrams measured. The missing binary interaction parameter for the ethanol + water system was estimated using the available experimental data for the isobaric VLE of the ethanol + water system at atmospheric pressure.[41] The k_{ij} value obtained (Table 4) provides a description of the experimental data with an average deviation of 0.1% for the bubble temperature.

Only the ethyl laurate/ethyl myristate + water and the ethyl laurate/ethyl myristate + ethanol interaction parameters, k_{ij}'s, were unavailable and were regressed from the ternary data. The values for the binary parameters are presented in Table 4, and the same set of interaction and cross-association binary parameters were use to model the LLE data at 298.15, 313.15, and 333.15 K.

The CPA descriptions of the experimental phase diagrams measured in this work at the various temperatures studied are reported in Figures 3 and 4. A good description of both the saturation curves and tie lines was obtained for both systems at all the temperatures studied.

Near the plait point, higher deviations between the experimental and calculated values were observed, with the CPA EoS predicting a somewhat larger region of two-liquid-phase coexistence. According to Zhou and Boocook,[42] the ester-rich phase obtained at the end of the ethanolysis reaction contains approximately 13% by mass of ethanol. Even considering that this value can oscillate as a function of the ethanol/oil ratio used during the reaction step, the ethanol composition in the ester-rich phase should not be much larger than the previously reported value. This means that the lower

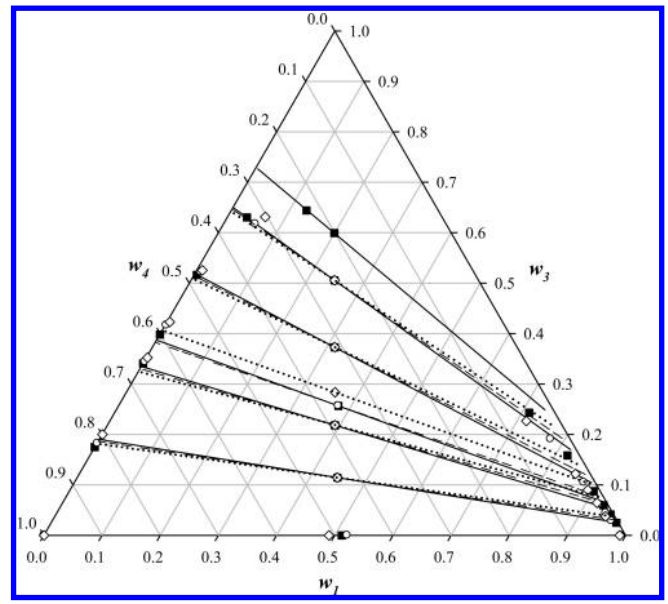

Figure 3. Liquid−liquid equilibrium for the system containing ethyl laurate (1) + ethanol (3) + water (4): experimental (■) and CPA results (—) at 298.15 K, experimental (○) and CPA results (--) at 313.15 K, and experimental (◊) and CPA results (•••) at 333.15 K.

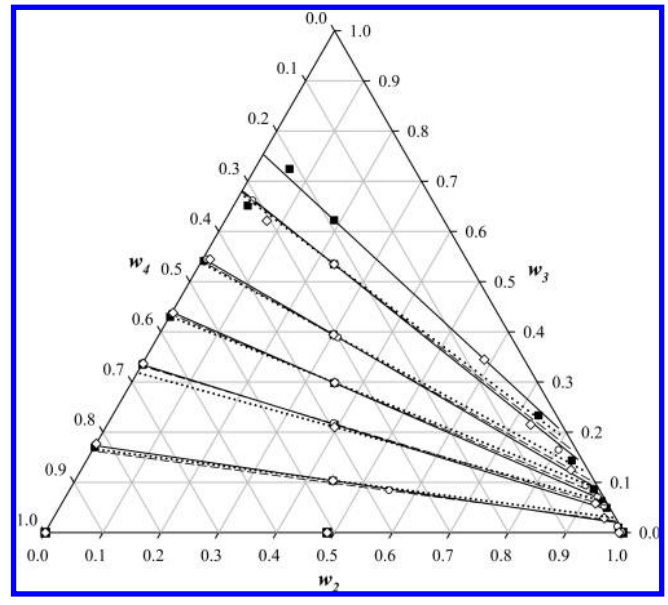

Figure 4. Liquid−liquid equilibrium for the system containing ethyl myristate (2) + ethanol (3) + water (4): experimental (■) and CPA results (—) at 298.15 K, experimental (○) and CPA results (--) at 313.15 K, and experimental (◊) and CPA results (•••) at 333.15 K.

Table 5. Average Deviations (AD) between the Experimental and Calculated Phase Compositions

system	CPA EoS		
	100AD ester in water-rich phase	100AD water in ester-rich phase	100AD[a]
ethyl laurate (1) + ethanol (3) + water (4) at 298.15 K	2.51	0.78	2.63
ethyl laurate (1) + ethanol (3) + water (4) at 313.15 K	1.45	0.81	1.66
ethyl laurate (1) + ethanol (3) + water (4) at 333.15 K	1.75	1.17	2.10
ethyl myristate (2) + ethanol (3) + water (4) at 298.15 K	1.26	0.95	1.58
ethyl myristate (2) + ethanol (3) + water (4) at 313.15 K	0.71	0.62	0.94
ethyl myristate (2) + ethanol (3) + water (4) at 333.15 K	1.66	5.27	5.53
average global deviation			2.80

[a] Average deviations calculated according to eq 13.

part of the phase splitting region in the equilibrium diagrams is the most important one for designing the water washing step of ethylic biodiesel, which is the part particularly well described by the CPA equation of state.

The results reported here represent a very stringent test of the predictive capability of the CPA EoS and the transferability of its binary parameters. The quality of the results obtained show that when reliable data are available, the parameters obtained from binary systems can be used with confidence for the estimation of ternary or high-order systems. The capacity of a single set of parameters to describe the phase diagrams across a temperature range is also remarkable. The reliability of the CPA in the description of the phase equilibrium of complex polar mixtures relevant to biodiesel production makes it the model of choice for the design, optimization, and operation of biodiesel production plants.

The average deviations between the experimental and calculated compositions in both phases are shown in Table 5. As can be seen in Table 5, most deviations are within the range from 0.9 to 2.6% and the average global deviation was 2.8%. If the tie lines closest to the plait point were not considered in estimating these deviations, the average global deviation decreased to a value of 1.64% and the deviations for most systems, with the single exception of ethyl myristate at 333.15 K, would be within the range from 0.9 to 1.2%. These results confirm that the larger deviations between the experimental and calculated values were concentrated in the phase splitting region close to the plait point.

Liquid−liquid equilibrium data for fatty systems containing ethanol and water were recently reported by Priamo et al.[43] and by Dalmolin et al.[44] These data were measured at 298.15 and 313.15 K and correlated with the NRTL equation. The average deviations (AD) reported for these systems were within the range from 0.5 to 1.6%. Although these deviations were slightly lower than those obtained in the present work, it should be considered that the NRTL equation requires nine binary interaction parameters at each temperature for a ternary system and that these parameters are specific for describing liquid−liquid equilibrium data.

In contrast, the correlation results obtained in the present work only required the adjustment of two new binary interaction parameters for each ternary system. The same set of parameters was used for the whole range of temperatures and for calculating the vapor−liquid as well as the liquid−liquid equilibrium data. Such an approach is particularly useful for designing biodiesel production, since the purification steps involve a series of vapor−liquid and liquid−liquid mass-transfer operations.

Conclusions

Equilibrium data were measured for the ethyl laurate/ethyl myristate + ethanol + water systems at 298.15, 313.15, and 333.15 K. The high ethanol distribution coefficients and very high solvent selectivities make water washing a very effective way of recovering ethanol from the ester-rich phase generated at the end of the ethanolysis reaction. The experimental data were correlated successfully with the cubic-plus-association equation of state (CPA EoS), and the average global deviation between the experimental data and the calculated compositions showed a value of 2.8%.

Acknowledgment

We acknowledge FAPESP (Grant 08/56258-8), CNPq (Grants 306250/2007-1 and 480992/2009-6), CAPES/PEC-PG, CAPES, and CAPES/PNPD for their financial support and scholarship. Mariana B. Oliveira acknowledges the *Fundação para a Ciência e a Tecnologia* for her Ph.D. (Grant SFRH/BD/29062/2006) scholarship.

Supporting Information Available: Table showing experimental data for binodal curves of ester ether (*i*) + ethanol (3) + water (4) at several temperatures. This material is available free of charge via the Internet at http://pubs.acs.org.

Nomenclature

K_d = distribution coefficient
S = solvent selectivity
a = energy parameter in the physical term
a_0, c_1 = parameters for calculating a
A_i = site A in molecule i
b = covolume
g = simplified hard-sphere radial distribution function
k_{ij} = binary interaction parameter
P = vapor pressure
R = gas constant
T = temperature
w = mass fraction
x = mole fraction
X_{A_i} = fraction of molecule i not bonded at site A
Z = compressibility factor

Greek Letters

β = association volume
Δ = association strength
ε = association energy
η = reduced fluid density
ρ = mole density

Subscripts

c = critical
i, j = pure component indexes
r = reduced
1 = ethyl laurate
2 = ethyl myristate
3 = ethanol
4 = water

Superscripts

assoc = association
calcd = calculated
exptl = experimental
phys = physical

Literature Cited

(1) Jones, J. C. On the Use of Ethanol in the Processing of Biodiesel Fuels (Letter to the Editor). *Fuel* **2010**, *89*, 1183.

(2) Marjanovic, A. V.; Stamenkovic, O. S.; Todorovic, Z. B.; Lazic, M. L.; Veljkovic, V. B. Kinetics of the Base-Catalyzed Sunflower Oil Ethanolysis. *Fuel* **2010**, *89*, 665.

(3) Alamu, O. J.; Waheed, M. A.; Jekayinfa, S. O. Effect of Ethanol-Palm Kernel Oil Ratio on Alkali-Catalyzed Biodiesel Yield. *Fuel* **2008**, *87*, 1529.

(4) Marchetti, J. M.; Miguel, V. U.; Errazu, A. F. Possible Methods for Biodiesel Production. *Renewable Sustainable Energy Rev.* **2007**, *11*, 1300.

(5) Teixeira, M. A. Babassu−A New Approach for an Ancient Brazilian Biomass. *Biomass Bioenergy* **2008**, *32*, 857.

(6) Firestone, D. *Physical and Chemical Characteristics of Oils, Fats and Waxes*, 2nd ed.; AOCS Press: Champaign, IL, 2006.

(7) Berrios, M.; Skelton, R. L. Comparison of Purification Methods for Biodiesel. *Chem. Eng. J.* **2008**, *144*, 459.

(8) Van Gerpen, J. Biodiesel Processing and Production. *Fuel Process. Technol.* **2005**, *86*, 1097.

(9) Karaosmanoğlu, F.; Cigizoglu, K. B.; Tuter, M.; Ertekin, S. Investigation of the Refining Step of Biodiesel Production. *Energy Fuels* **1996**, *10*, 890.

(10) Tizvar, R.; McLean, D. D.; Kates, M.; Dubé, M. A. Liquid−Liquid Equilibria of the Methyl Oleate−Glycerol−Hexane−Methanol System. *Ind. Eng. Chem. Res.* **2008**, *47*, 443.

(11) Liu, X.; Piao, X.; Wang, Y.; Zhu, S. Liquid−Liquid Equilibrium for Systems of (Fatty Acid Ethyl Esters + Ethanol + Soybean Oil and Fatty Acid Ethyl Esters + Ethanol + Glycerol). *J. Chem. Eng. Data* **2008**, *53*, 359.

(12) Follegatti-Romero, L. A.; Lanza, M.; da Silva, C. A. S.; Batista, E. A. C. Meirelles, A. J. A. Mutual Solubility of Pseudobinary Systems Containing Vegetable Oils and Anhydrous Ethanol from (298.15 to 333.15) K. *J. Chem. Eng. Data* **2010**, *55*, 2750.

(13) Lanza, M.; Sanaiotti, G.; Batista, E.; Poppi, R. J.; Meirelles, A. J. A. Liquid−Liquid Equilibrium Data for Systems Containing Vegetable Oils, Anhydrous Ethanol, and Hexane at (313.15, 318.15, and 328.15) K. *J. Chem. Eng. Data* **2009**, *54*, 1850.

(14) Kontogeorgis, G. M.; Yakoumis, I. V.; Meijer, H.; Hendriks, E.; Moorwood, T. Multicomponent Phase Equilibrium Calculations for Water-Methanol-Alkane Mixtures. *Fluid Phase Equilib.* **1999**, *160*, 201.

(15) Andreatta, A. E.; Casás, L. M.; Hegel, P.; Bottini, S. B.; Brignole, E. A. Phase Equilibria in Ternary Mixtures of Methyl Oleate, Glycerol, and Methanol. *Ind. Eng. Chem. Res.* **2008**, *47*, 5157.

(16) Lanza, M.; Borges Neto, W.; Batista, E.; Poppi, R. J.; Meirelles, A. J. A. Liquid−Liquid Equilibrium Data for Reactional Systems of Ethanolysis at 298.3 K. *J. Chem. Eng. Data* **2008**, *53*, 5.

(17) Kontogeorgis, G. M.; Michelsen, M. L.; Folas, G. K.; Derawi, S.; von Solms, N.; Stenby, E. H. Ten Years with the CPA (Cubic-Plus-Association) Equation of State. Part 1. Pure Compounds and Self-Associating Systems. *Ind. Eng. Chem. Res.* **2006**, *45*, 4855.

(18) Kontogeorgis, G. M.; Michelsen, M. L.; Folas, G. K.; Derawi, S.; von Solms, N.; Stenby, E. H. Ten Years with the CPA (Cubic-Plus-Association) Equation of State. Part 2. Cross-Associating and Multicomponent Systems. *Ind. Eng. Chem. Res.* **2006**, *45*, 4869.

(19) Kontogeorgis, G. M.; Voutsas, E. C.; Yakoumis, I. V.; Tassios, D. P. An Equation of State for Associating Fluids. *Ind. Eng. Chem. Res.* **1996**, *35*, 4310.

(20) Michelsen, M. L.; Hendriks, E. M. Physical Properties from Association Models. *Fluid Phase Equilib.* **2001**, *180*, 165.

(21) Voutsas, E. C.; Boulougouris, G. C.; Economou, I. G.; Tassios, D. P. Water/Hydrocarbon Phase Equilibria Using the Thermodynamic Perturbation Theory. *Ind. Eng. Chem. Res.* **2000**, *39*, 797.

(22) Wu, J. Z.; Prausnitz, J. M. Phase Equilibria for Systems Containing Hydrocarbons, Water, and Salt: An Extended Peng−Robinson Equation of State. *Ind. Eng. Chem. Res.* **1998**, *37*, 1634.

(23) Muller, E. A.; Gubbins, K. E. Molecular-Based Equations of State for Associating Fluids: A Review of Saft and Related Approaches. *Ind. Eng. Chem. Res.* **2001**, *40*, 2193.

(24) Folas, G. K.; Gabrielsen, J.; Michelsen, M. L.; Stenby, E. H.; Kontogeorgis, G. M. Application of the Cubic-Plus-Association (CPA) Equation of State to Cross-Associating Systems. *Ind. Eng. Chem. Res.* **2005**, *44*, 3823.

(25) Voutsas, E. C.; Yakoumis, I. V.; Tassios, D. P. Prediction of Phase Equilibria in Water/Alcohol/Alkane Systems. *Fluid Phase Equilib.* **1999**, *160*, 151.

(26) Oliveira, M. B.; Pratas, M. J.; Marrucho, I. M.; Queimada, A. J.; Coutinho, J. A. P. Description of the Mutual Solubilities of Fatty Acids and Water with the CPA EoS. *AIChE J.* **2009**, *55*, 1604.

(27) Oliveira, M. B.; Teles, A. R. R.; Queimada, A. J.; Coutinho, J. A. P. Phase Equilibria of Glycerol Containing Systems and Their Description with the Cubic-Plus-Association (CPA) Equation of State. *Fluid Phase Equilib.* **2009**, *280*, 22.

(28) Folas, G. K.; Kontogeorgis, G. M.; Michelsen, M. L.; Stenby, E. H. Application of the Cubic-Plus-Association (CPA) Equation of State to Complex Mixtures with Aromatic Hydrocarbons. *Ind. Eng. Chem. Res.* **2006**, *45*, 1527.

(29) Oliveira, M. B.; Coutinho, J. A. P.; Queimada, A. J. Mutual Solubilities of Hydrocarbons and Water with the CPA EoS. *Fluid Phase Equilib.* **2007**, *258*, 58.

(30) Oliveira, M. B.; Varanda, F. R.; Marrucho, I. M.; Queimada, A. J.; Coutinho, J. A. P. Prediction of Water Solubility in Biodiesel with the CPA Equation of State. *Ind. Eng. Chem. Res.* **2008**, *47*, 4278.

(31) Huang, S. H.; Radosz, M. Equation of State for Small, Large, Polydisperse, and Associating Molecules. *Ind. Eng. Chem. Res.* **1990**, *29*, 2284.

(32) Taylor, B. N.; Kuyatt, C. E., *Guidelines for the Evaluation and Expression of Uncertainty in NIST Measurement Results*, Technical Note 1297 for NIST; National Institute of Standards and Technology: Gaithersburg: MD, 1994.

(33) Marcilla, A.; Ruiz, F.; Garcia, A. N. Liquid-Liquid-Solid Equilibria of the Quaternary System Water-Ethanol-Acetone-Sodium Chloride at 25-Degrees-C. *Fluid Phase Equilib.* **1995**, *112*, 273.

(34) da Silva, C. A. S.; Sanaiotti, G.; Lanza, M.; Follegatti-Romero, L. A.; Meirelles, A. J. A.; Batista, E. A. C. Mutual Solubility for Systems Composed of Vegetable Oil + Ethanol + Water at Different Temperatures. *J. Chem. Eng. Data* **2010**, *55*, 440.

(35) Oliveira, M. B.; Queimada, A. J.; Coutinho, J. A. P. Modeling of Biodiesel Multicomponent Systems with the Cubic-Plus-Association (CPA) Equation of State. *Ind. Eng. Chem. Res.* **2010**, *49*, 1419.

(36) Oliveira, M. B.; Freire, M. G.; Marrucho, I. M.; Kontogeorgis, G. M.; Queimada, A. J.; Coutinho, J. A. P. Modeling the Liquid−Liquid Equilibria of Water + Fluorocarbons with the Cubic-Plus-Association Equation of State. *Ind. Eng. Chem. Res.* **2007**, *46*, 1415.

(37) Oliveira, M. B.; Queimada, A. J.; Coutinho, J. A. P. Prediction of Near and Supercritical Fatty Acid Ester + Alcohol Systems with the CPA EoS. *J. Supercrit. Fluids* **2010**, *52*, 241.

(38) Pratas, M. J.; Freitas, S.; Oliveira, M. B.; Monteiro, S. C.; Lima, A. S.; Coutinho, J. A. P. Densities and Viscosities of Fatty Acid Methyl and Ethyl Esters. *J. Chem. Eng. Data* **2010**, *55*, 3983.

(39) Oliveira, M. B.; Marrucho, I. M.; Coutinho, J. A. P.; Queimada, A. J. Surface Tension of Chain Molecules Through a Combination of the Gradient Theory with the CPA EoS. *Fluid Phase Equilib.* **2008**, *267*, 83.

(40) Oliveira, M. B.; Miguel, S. I.; Queimada, A. J.; Coutinho, J. A. P. Phase Equilibria of Ester + Alcohol Systems and Their Description with the Cubic-Plus-Association Equation of State. *Ind. Eng. Chem. Res.* **2010**, *49*, 3452.

(41) Iwakabe, K.; Kosuge, H. Isobaric Vapor-Liquid-Liquid eEquilibria with a Newly Developed Still. *Fluid Phase Equilib.* **2001**, *192*, 171.

(42) Zhou, W.; Boocock, D. G. B. Phase Distributions of Alcohol, Glycerol, and Catalyst in the Transesterification of Soybean Oil. *J. Am. Oil Chem. Soc.* **2006**, *83*, 1047.

(43) Priamo, W. L.; Lanza, M.; Meirelles, A. J. A.; Batista, E. A. C. Liquid−Liquid Equilibrium Data for Fatty Systems Containing Refined Rice Bran Oil, Oleic Acid, Anhydrous Ethanol, and Hexane. *J. Chem. Eng. Data* **2009**, *54*, 2174.

(44) Dalmolin, I.; Lanza, M.; Meirelles, A. J. A.; Batista, E. A. C. Liquid−Liquid Equilibrium Data for Systems Containing Refined Rice Bran Oil, Anhydrous ethanol, Water, and Hexane. *J. Chem. Eng. Data* **2009**, *54*, 2182.

Received for review July 28, 2010
Revised manuscript received September 30, 2010
Accepted October 13, 2010

IE101611J